



Facile and sensitive multi quantitative determination of tamsulosin and dutasteride in commercial tablet based on citrate-capped gold nanoparticles along with smart chemometrics-assisted spectrophotometric methods

Ghasem Mahmoudi · Mahmoud Reza Sohrabi · Fereshteh Motiee

Received: 3 February 2024 / Accepted: 11 June 2024 / Published online: 27 June 2024
© The Author(s), under exclusive licence to Springer Nature B.V. 2024

Abstract In this work, a simple colorimetric method based on the gold nanoparticles (AuNPs) using its localized surface plasmon resonance (LSPR) was proposed for the simultaneous determination of tamsulosin (TAM) and dutasteride (DTS) in pharmaceutical formulation. The aggregation of citrate-capped AuNPs was observed in the presence of TAM and DTS, which led to a change in color from red to gray. Also, the absorbance was shifted from 524 to 674 nm. The formation and size of synthesized AuNPs before and after aggregation were evaluated by transmission electron microscopy (TEM) and dynamic light scattering (DLS), which were found to be 11.49 and 122.1 nm, respectively. The colorimetric method was validated in the concentration range of 50–200 µg/L, where it revealed good linearity ($R^2=0.9958$ for TAM and $R^2=0.9912$ for DTS). The limit of detection (LOD) and limit of quantitation (LOQ) were found to be 21.08, 21.82 µg/L and 63.90, 66.12 µg/L for TAM and DTS, respectively. Radial basis function neural network (RBF-NN) and fuzzy inference system (FIS) were coupled with this approach for the simultaneous estimation of both components. The mean recovery percentage of the RBF model was higher than 99.99% for both components, as well as root mean square error (RMSE)

values were 3.69×10^{-13} and 1.75×10^{-13} for TAM and DTS, respectively. In the FIS model, the mean recovery was 99.15% and 101.76% for TAM and DTS, respectively, while RMSE was lower than 3.2. These methods were compared with high-performance liquid chromatography (HPLC) through an analysis of variance (ANOVA) test. This colorimetric method can be an appropriate choice for the determination of drug contents in pharmaceutical and biological samples.

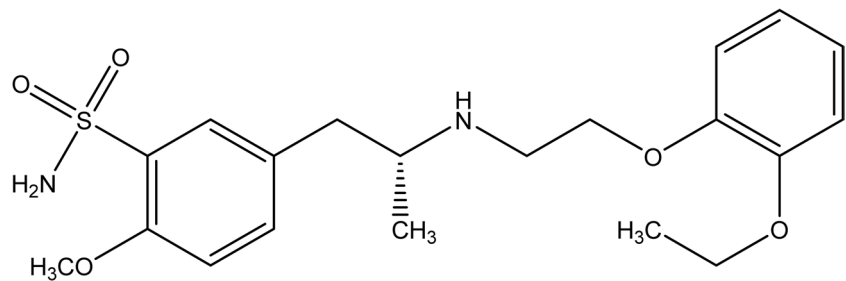
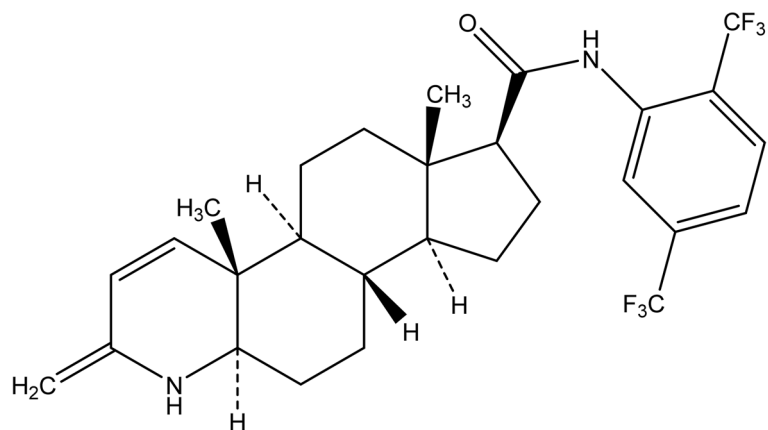
Keywords Gold nanoparticles · Colorimetric · Surface plasmon resonance · Anti-cancer prostate drugs · Chemometrics

Introduction

One of the most common non-malignant conditions in older men is benign prostatic hyperplasia (BPH) [1]. It indicates a non-cancerous growth of the prostate that occurs in old age. It has been estimated that a percentage of men over 60 years old (33%) have BPH. Nocturia, intermittent urinary retention, and kidney failure are symptoms of BPH [2]. Also, a higher percentage of this disease is assigned to men over 80 years old [3].

Groups of alpha-adrenergic antagonist drugs and 5- α -reductase inhibitors can be used to treat BPH. Tamsulosin (TAM) (Scheme 1a) as an alpha-adrenergic antagonist prevents the contraction of the smooth

G. Mahmoudi · M. R. Sohrabi (✉) · F. Motiee
Department of Chemistry, Islamic Azad University, North
Tehran Branch, Tehran, Iran
e-mail: Sohrabi.m46@yahoo.com

Scheme 1 Chemical structure of **a** TAM and **b** DTS**(a)****(b)**

muscle of the prostate, which can decrease resistance to bladder neck contraction and urethra in men [4, 5]. Dutasteride (DTS) (Scheme 1b) is a 5 α -reductase inhibitor, which is known as a type of anti-androgen. It is a selective inhibitor of both type 1 and type 2 of 5 α -reductase (5-AR) enzyme. DTS is prescribed for the treatment of BPH, as well as it can reduce the production of 5 α -dihydrotestosterone (DHT) in the prostate gland [6–8]. These drugs are used alone or in combination with each other. The combination of these two drugs reduces the size of the prostate through various mechanisms. The prostate smooth muscle tone is decreased by α -blockers in the short-term and the prostate volume is reduced by 5ARIs over the long term [9].

A literature survey indicates that some analytical techniques, including reversed-phase high-performance liquid chromatography (RP-HPLC) [10, 11], thin-layer chromatography (TLC) [12, 13], and liquid chromatography-tandem mass spectrometry

(LC–MS–MS) [14] have been developed for simultaneous determination of TAM and DTS in different samples. However, chromatography techniques have several limitations, such as the need in long runtime or large sample volumes [15]. In addition, expensive sample pre-treatment processes and the usage of expensive analytical instrumentation, which are not available in all laboratories, are the other drawbacks of these methods [16]. Compared to the aforesaid methods, the colorimetric approach has become extremely attractive owing to its ease, simplicity, and inexpensive. Also, the response related to the colorimetry is easy to detect with the naked eye without any complicated instrumentation [17, 18].

Gold nanoparticles (AuNPs) have been widely used for colorimetric analysis due to their biocompatibility, great size and distance-dependent surface plasmon resonance (SPR) features, and high molar extinction coefficients, which could display visible color change via aggregation or growth of NPs,

even at low concentrations [19–21]. The greatest benefit of AuNPs based on colorimetric detection is their changing color in various sizes, which leads to the recognition of diverse analytes. This procedure is based on the two-way approach: (1) the change in color from red to blue/purple can be observed during aggregation and (2) a change from blue/purple to red exists in separation. It can be said that there is a change in SRP peak absorption between the dispersed and aggregation modes of AuNPs, which causes color change [22].

The colorimetric method coupled with the chemometric approach can have good potential for the simultaneous quantification determination of drugs [23]. Artificial intelligence techniques can be useful, including radial basis function neural network (RBF-NN) and fuzzy inference system (FIS). The RBF-NN was represented by Broomhead and Lowe in 1988. It is known as an easy and flexible regression model, which can be introduced as a feedforward neural network (FF-NN) with one hidden layer [24]. One chemometric approach that possesses the potential to deal with an assessment of imprecise and uncertain data is fuzzy inference systems (FIS), which is superior to multi-criteria analysis (MCA) techniques [25].

In this study, a simple, fast, low-cost approach, without the need sample preparation process and expensive apparatus was proposed for the simultaneous determination of TAM and DTS in their binary mixtures in a scale of $\mu\text{g/L}$. The mentioned features are the advantages of the suggested method compared to the chromatographic techniques. This method is based on the synthesized AuNPs and their aggregation in the presence of the drug. RBF-NN and FIS as chemometrics methods were applied along with the colorimetric technique for solving overlap problem of components. Finally, RBF-NN and FIS were compared with the HPLC using the analysis of variance (ANOVA) test.

Theoretical background

RBF neural network

RBF-NN has a good performance, which includes three layers. The distribution of input to the nodes related to the hidden layer is performed using the input layer. The connection of each node with a

center is evident in the hidden layer. The node dimension is equal to the number of input variables. A nonlinear transformation is performed with the hidden layer, and the mapping of the input space to a new high-dimensional space occurs with this layer. After setting the network weight, the generation of the output of the RBF-NN happens through the linear combination of hidden node responses. The RBF is the activation function of the hidden layer. It is a scalar function, which is described as a function of the radial distance between the data center and the sample. Mapping the low-dimensional nonlinear separable input into a high-dimensional linear separable space is done by the radial function. The response of the activation function of the hidden layer node to the input is local. The proximity of the input to the central range of the basis function leads to a larger output by the hidden layer node. Moving away from the center point decreases the output exponentially [26, 27].

FIS model

The FIS as a rule-based system includes three sections: (1) a rule base comprising a collection of fuzzy If–Then rules; (2) a database that describes the membership function (MF) related to the input–output variables; and (3) a reasoning process that sums the output from fuzzy rules to obtain a proper conclusion [28]. The input variables can be shown either as crisp values or a fuzzy set, while the output is generally presented as a fuzzy set. The defuzzification step is required to take decisions based on the FIS output in the fuzzy output. A nonlinear mapping between the input and output space in modeling mode can be facilitated using If–Then rules. The entire input–output space is divided into a number of local regions via fuzzy rules, and the local behavior of the nonlinear mapping is specified by each rule. Hence, the number of fuzzy rules determines the performance of FIS [25]. Two approaches, including Mamdani and the Takagi–Sugeno are defined for the FIS [29, 30]. There are three processes containing fuzzification of the input variables, logic decision, and defuzzification of the FIS output for the Mamdani method. There is no explicit defuzzification process in the Takagi–Sugeno method [25].

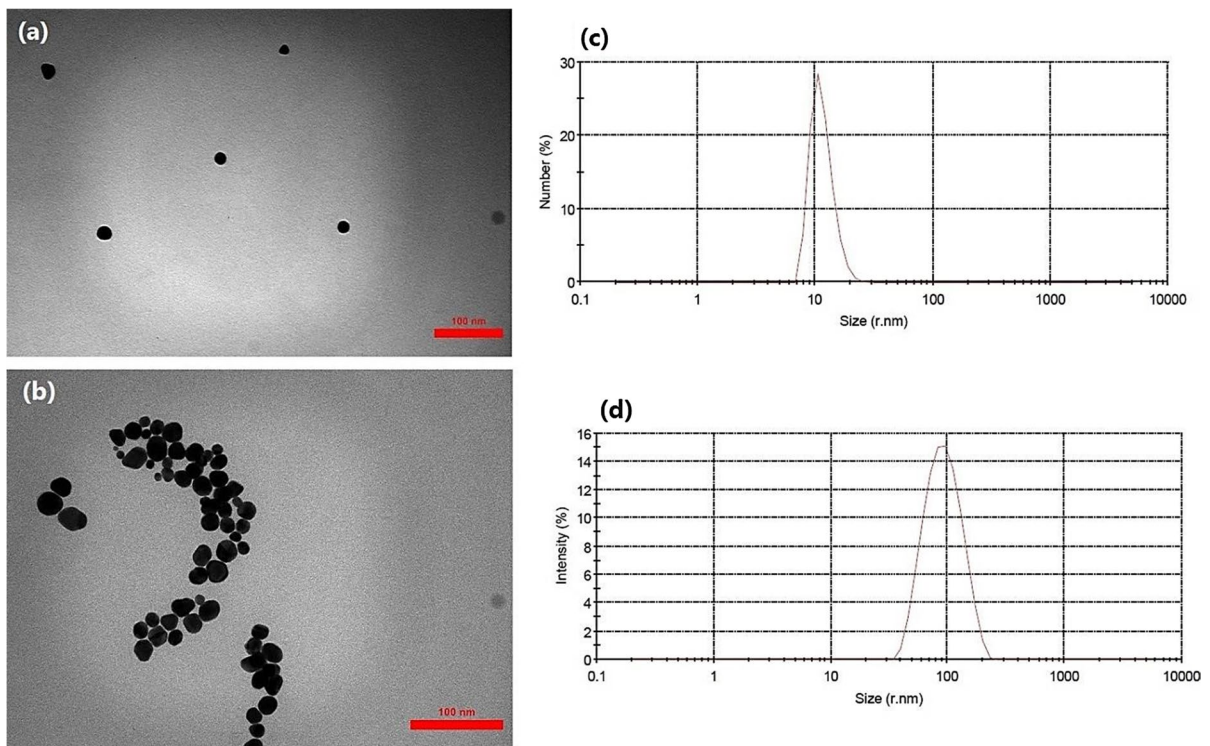


Fig. 1 TEM images of **a** AuNPs and **b** AuNPs + drug. DLS spectra in the **c** absence and **d** presence of drug

Materials and methods

Materials

Pure TAM (99.9%) was provided by Darou Pakhsh Pharma Chem Co. Pure DTS (99.9%) was prepared by Zahravi Co. Avolosin capsule (0.4 mg TAM and 0.5 mg DTS) was purchased from Tasnim Co. Ethanol, tetrachloroauric(III) acid trihydrate ($\text{HAuCl}_4 \cdot 3\text{H}_2\text{O}$), and trisodium citrate ($\text{Na}_3\text{C}_6\text{H}_5\text{O}_7$) were procured from Merck.

Preparation of AuNPs

0.0214 g of $\text{HAuCl}_4 \cdot 3\text{H}_2\text{O}$ was dissolved in double-distilled water and made up to a volume of 100 mL in a volumetric flask. Then, the solution was transferred to a 250-mL Erlenmeyer flask and stirred with a magnetic stirrer at a rate of 400 rpm. At the same time, the solution was heated to boiling. While boiling, a watch glass containing some ice was placed

on the Erlenmeyer flask to prevent the evaporation of the solution. After boiling, in 4 to 5 steps, 1 mL of trisodium citrate solution (1.1%) was added each time until the color change from light yellow to gray and then wine-red was observed. Heating and stirring continued for 10 min, and then the solution was cooled at room temperature. The obtained AuNPs were stored in dark containers at 4 °C and away from light. Different concentrations of AuNPs were prepared from the stock solution with a concentration of 5×10^{-4} mol/L.

Preparation of standard solution

0.1 g of pure TAM and DTS were dissolved separately in ethanol and made up to volume in a 100-mL volumetric flask. In order to prepare standard solutions with different concentrations, the dilution of the stock solutions of each component was done, and a certain amount of AuNPs was added to each of the solutions and adjusted to volume. Finally, the absorption of

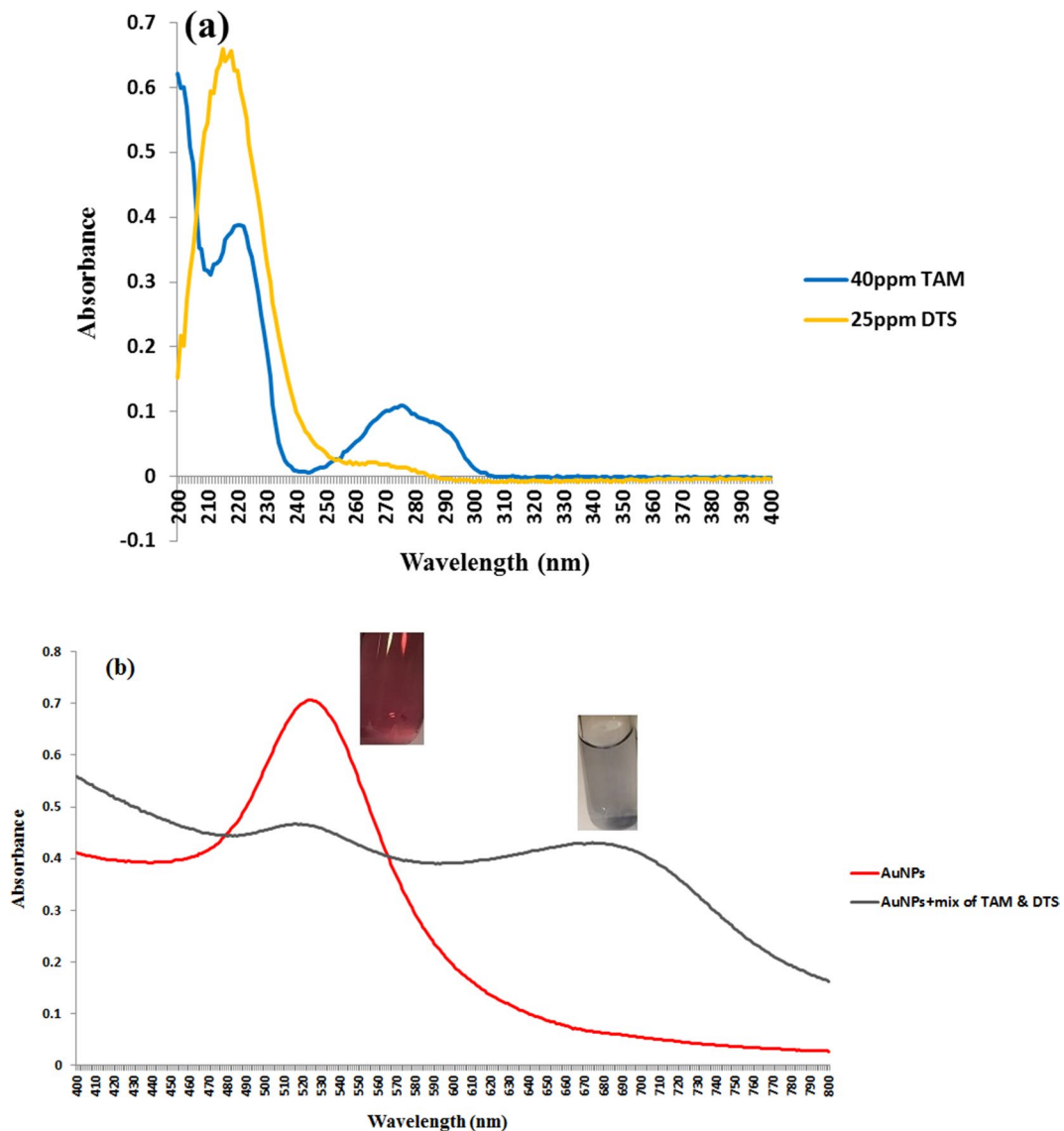


Fig. 2 **a** The overlay spectrum of TAM and DTS and **b** UV-Vis spectra of AuNPs and AuNPs + drug

these solutions was recorded using T90 + double beam UV-visible from PG Instruments Ltd.

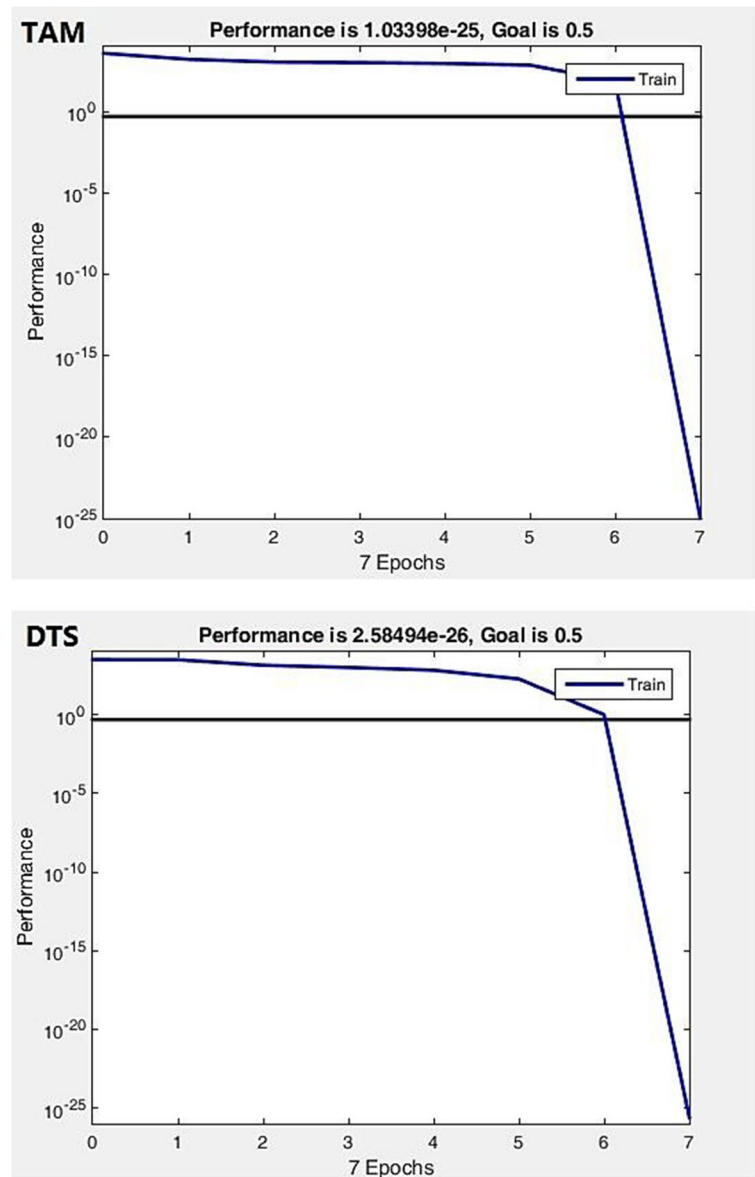
Preparation of mixtures

Various concentrations of TAM and DTS of stock solutions along with a certain amount of AuNPs were used to prepare eight mixtures to evaluate the validity of the RBF and FIS approaches. Afterward, their absorption was recorded.

Preparation of pharmaceutical sample

Ten tablets were weighed and powdered separately. Then, the average weight equivalent of one tablet (1.1 g) was dissolved in ethanol. The solution was placed in an ultrasonic device for 20 min to completely dissolve. Afterward, it was placed in a centrifuge at a rate of 400 rpm for 11 min and the supernatant was passed through filter paper. Then, it was transferred to a 100-mL volumetric flask and made

Fig. 3 MSE versus the number of epochs for TAM and DTS in RBF-NN model



up to the volume. A specific amount of AuNPs was added to the resulting solution, and its absorption was recorded under optimal conditions.

Chromatographic conditions

HPLC Agilent 1200 equipped with an ultraviolet (UV) detector at 274 nm was used to analyze the real sample. Chromatographic separation was conducted using a column Agilent zorbax SB-C18 (15 cm, 3.5 μ m) with a temperature of 25 °C. The mobile

phase consists of water and acetonitrile (30:70 v/v). Its flow rate was 1 mL/min. The injection volume was 20 μ L.

Results and discussion

Characterization

In order to identify the structure and morphology of AuNPs and AuNPs in combination with the drug,

Fig. 4 Predicted values ($\mu\text{g/L}$) versus actual values ($\mu\text{g/L}$) for TAM and DTS in RBF-NN model

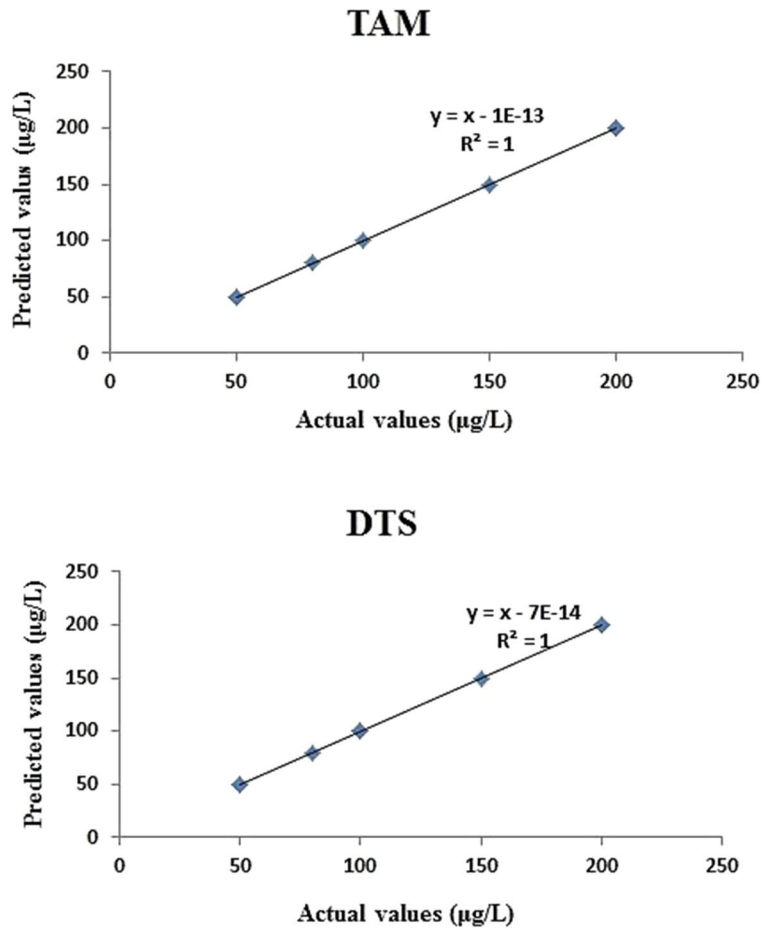


Table 1 Obtained recovery, mean recovery, and RMSE of TAM and DTS in RBF-NN model

| Sample no | Actual ($\mu\text{g/L}$) | | Predicted ($\mu\text{g/L}$) | | Recovery (%) | |
|---------------|----------------------------|-----|-------------------------------|--------|------------------------|------------------------|
| | TAM | DTS | TAM | DTS | TAM | DTS |
| 1 | 50 | 50 | 50.00 | 50.00 | 100.00 | 100.00 |
| 2 | 200 | 50 | 200.00 | 49.99 | 100.00 | 99.99 |
| 3 | 150 | 80 | 150.00 | 80.00 | 100.00 | 100.00 |
| 4 | 80 | 100 | 80.00 | 100.00 | 100.00 | 100.00 |
| 5 | 200 | 100 | 200.00 | 99.99 | 100.00 | 99.99 |
| 6 | 100 | 150 | 99.999 | 150.00 | 99.99 | 100.00 |
| 7 | 50 | 200 | 50.00 | 200.00 | 100.00 | 100.00 |
| 8 | 200 | 200 | 200.00 | 200.00 | 100.00 | 100.00 |
| Mean recovery | | | | | 99.99 | 99.99 |
| RMSE | | | | | 3.69×10^{-13} | 1.75×10^{-13} |

TEM analysis (PHILIPS-CM120, Netherlands) was used. The spherical and well-dispersed state of AuNPs is shown in Fig. 1(a). After adding the drug, the aggregation of NPs can be observed (Fig. 1b). Dynamic light scattering (DLS) (MALVERN-ZEN3600, England) was applied to determine the particle size

distribution of NPs before and after adding the drug. The average size was found to be 11.49 nm (Fig. 1c) and 122.1 nm (Fig. 1d) for AuNPs and AuNPs + drug, respectively. This increase in the size indicated that NPs were gradually aggregated in the presence of the drug.

Table 2 The results obtained related to the absorption of eight mixtures by PCA method

| No | Input 1 | Input 2 |
|----|-------------|--------------|
| 1 | 2.365596241 | -3.624421828 |
| 2 | 5.32356180 | -2.533441604 |
| 3 | 5.838344214 | -3.186078852 |
| 4 | 4.68272458 | -4.230858235 |
| 5 | 5.078018941 | -3.548296515 |
| 6 | 3.411659814 | -4.346467391 |
| 7 | 5.624160931 | -5.82106055 |
| 8 | 5.326789326 | -3.835448843 |

Spectral characteristics

Figure 2 (a) exhibits the UV spectra of TAM (40 µg/mL) and DTS (25 µg/mL). Owing to the strong overlapping of both components, direct and simultaneous

spectrophotometric determination of one component in the presence of the other one is not possible. Hence, RBF-NN and FIS methods were used to overcome this problem in the mixtures comprising TAM and DTS.

The UV-Vis spectrum of synthesized AuNPs displays a SPR band at 524 nm (Fig. 2b). By adding the drug, the absorption intensity was diminished. On the other hand, a remarkable increase in peak wavelength (λ_{max}) around 674 nm was observed. In addition, a color change from red to gray occurred due to the aggregation of AuNPs (Fig. 2b).

RBF-NN results

In this network, the input includes a matrix with a dimension of 401×8 containing absorbance of eight

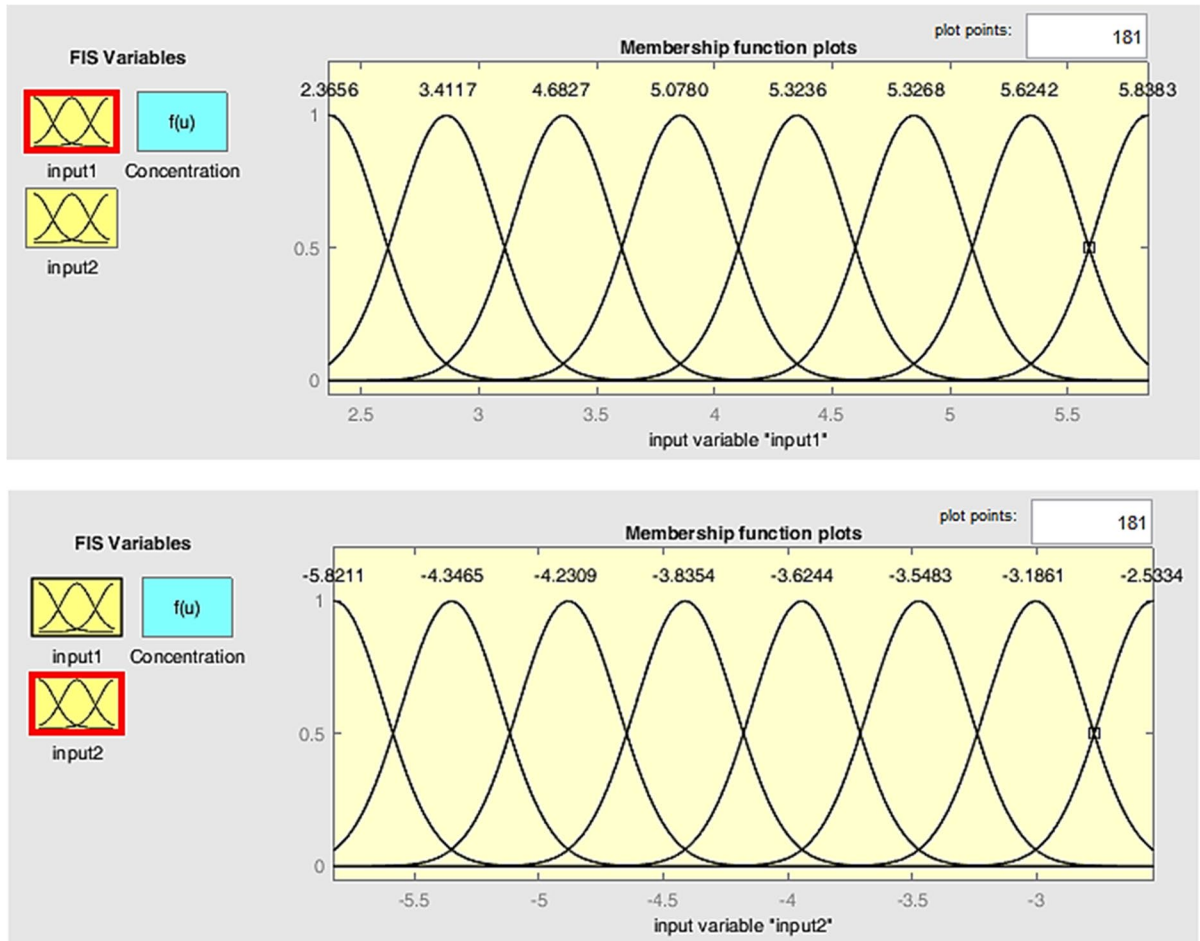


Fig. 5 Gaussian membership functions related to the inputs of FIS model

Table 3 If–Then rules of TAM and DTS in a FIS model

| No | TAM | | | DTS | | |
|----|-------------|--------------|---------------|-------------|--------------|---------------|
| | Input 1 | Input 2 | Concentration | Input 1 | Input 2 | Concentration |
| 1 | 2.365596241 | −3.624421828 | 50 | 2.365596241 | −3.624421828 | 50 |
| 2 | 5.32356180 | −2.533441604 | 200 | 5.32356180 | −2.533441604 | 50 |
| 3 | 5.838344214 | −3.186078852 | 150 | 5.838344214 | −3.186078852 | 80 |
| 4 | 4.68272458 | −4.230858235 | 80 | 4.68272458 | −4.230858235 | 100 |
| 5 | 5.078018941 | −3.548296515 | 200 | 5.078018941 | −3.548296515 | 100 |
| 6 | 3.411659814 | −4.346467391 | 100 | 3.411659814 | −4.346467391 | 150 |
| 7 | 5.624160931 | −5.82106055 | 50 | 5.624160931 | −5.82106055 | 200 |
| 8 | 5.326789326 | −3.835448843 | 200 | 5.326789326 | −3.835448843 | 200 |

mixtures in the range of 400–800 nm. The actual (experimental) concentrations of TAM and DTS existing in the mixtures were considered as RBF-NN targets with a matrix dimension of 8 × 1. In order to write the RBF-NN in a MATLAB R2020b software environment, several parameters such as degree of freedom (df), goal, spread, and the number of neurons (nm) were selected. The degree of freedom was considered equal to 1 (df=1) so that one neuron is added to the set in each epoch if the network error increases. The error of the network was chosen to be 0.5 (goal=0.5) to assess the efficiency of the RBF model for predicting concentrations. The spread value was selected 0.9, which was in the range of absorption of mixtures. The “mn” value was 8 because of the eight mixtures made. After writing this program and run of this model, performance (mean square error (MSE)) versus epochs was separately plotted for each component (Fig. 3). Low MSE values (TAM=1.033 × 10^{−25} and DTS=2.854 × 10^{−26}) reveal the high efficiency of this network for the prediction of concentration. The goodness-of-fit of predicted values vs. actual values can be studied using the coefficient of determination (R²) (Fig. 4). The R² is a statistical measure of how close the predictions are to the actual data. An R² equal to 1 was obtained for both components, indicating a perfect fit of regression predictions to the data. The non-scattering of the points indicates the closeness of the predicted values to the experimental values. Considering the lack of scattering of points, it can be said that the values obtained from the software are very close to the laboratory values. The accuracy of this model was determined using recovery percentage and mean recovery (Table 1). The percentage of recoveries showed up to 13 decimal digits in Excel software, which is reported here to two decimal

digits. These values are close to 100, indicating the great accuracy of the RBF approach. Low root mean square error (RMSE) (Eq. 1) (TAM=3.69 × 10^{−13} and DTS=1.75 × 10^{−13}) represented the high potential of this model for the prediction of concentrations.

$$RMSE = \sqrt{\frac{\sum_{i=1}^n (y_{pred} - y_{obs})^2}{n}} \tag{1}$$

where the predicted and the actual values of the concentrations are shown by y_{pred} and y_{obs}, respectively; the number of mixtures is denoted by “n” [31].

FIS results

In the first step, principal component analysis (PCA) was used to reduce the dimension of absorption of eight mixtures. Two dimensions were obtained, which write as input 1 and input 2 (Table 2). These two columns along with concentrations related to each component in mixtures were individually imported to the MATLAB environment. The Sogno system was applied to the data. Afterward, the Gaussian membership function (MF) was considered among various MFs (trapezoidal, triangular, etc.). The data were sorted from smallest to largest, which is shown on the peaks (Fig. 5). In addition, the sorting of concentration values of both components in eight mixtures was separately performed from small to large. In the next step, the rule of each MF (If–Then rule) was written (Table 3). For example, the second rule is stated as follows:

If input 1 is equal to 5.32356180 and input 2 is equal to −2.533441604, then the output will be equal to 200 and 50 μg/L for TAM and DTS,

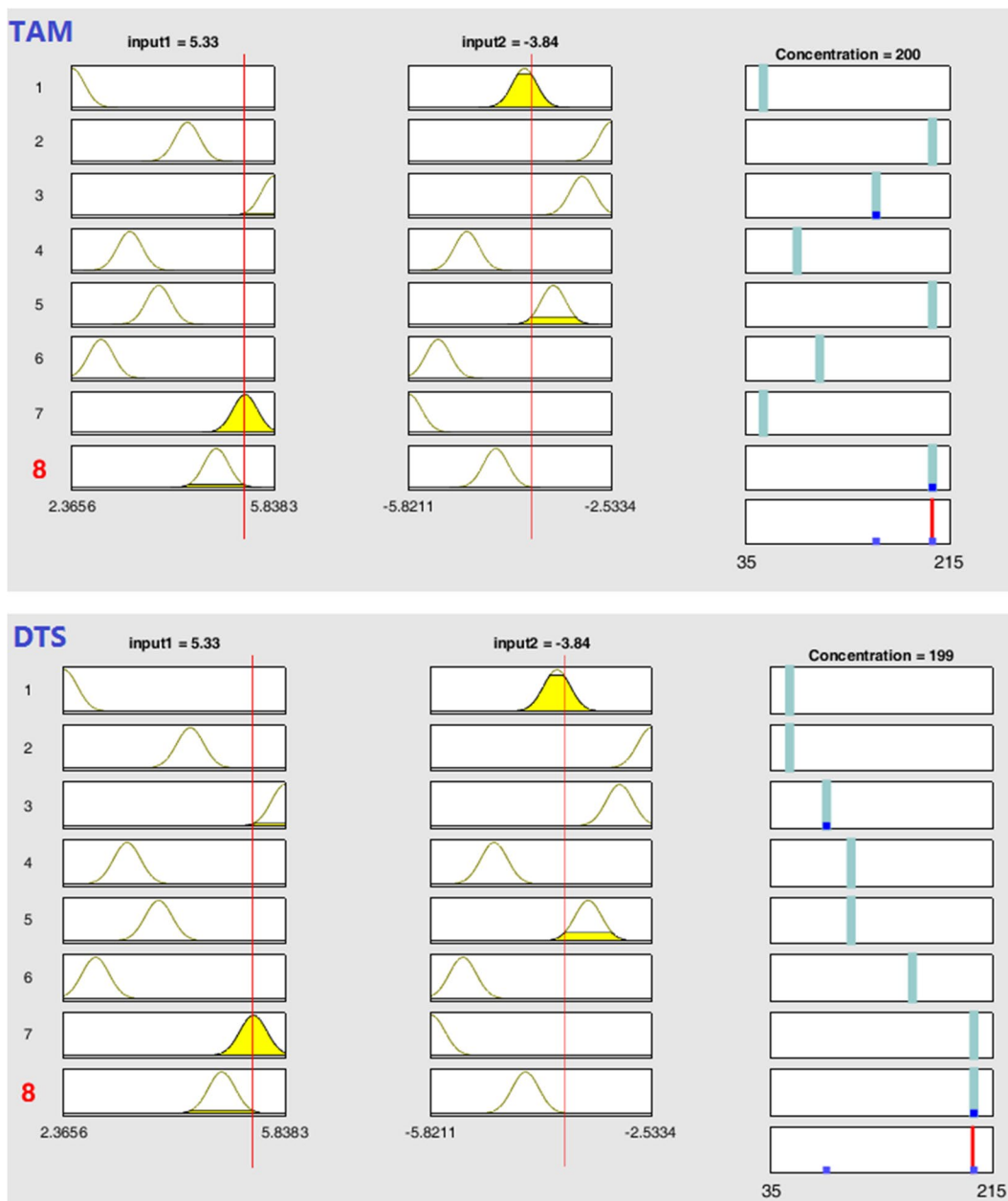


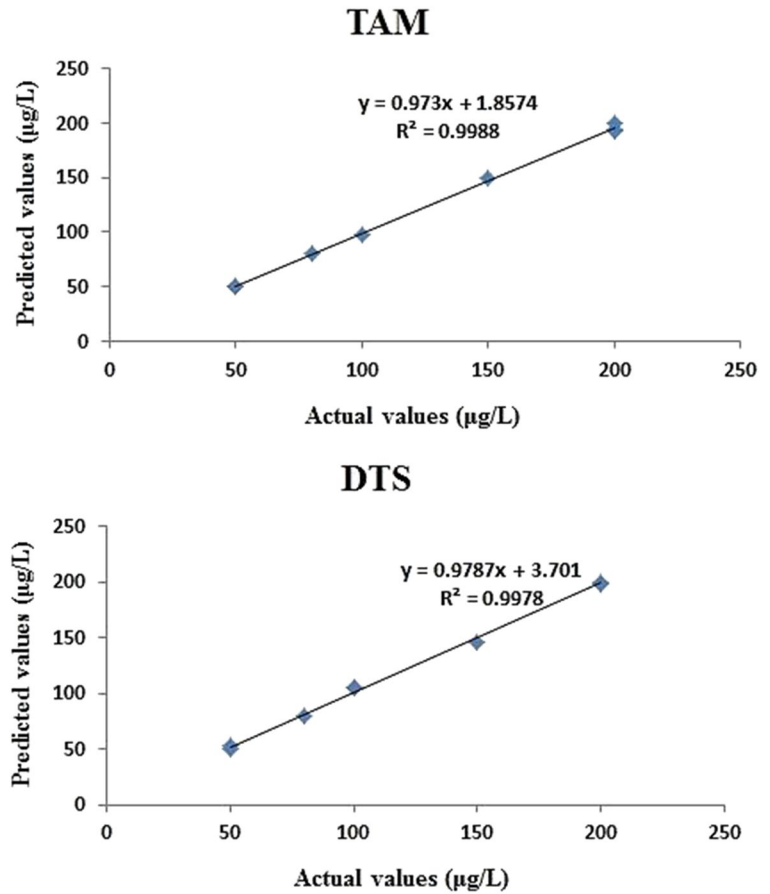
Fig. 6 The rule viewers for the prediction of TAM and DTS concentrations of FIS model

respectively. Other rules are also expressed in the same way. After entering the next stage, inputs were denoted by column 1 and column 2. The predicted concentration of each row (rule) was achieved via a run of this model. These predicted values are shown in the third column (Fig. 6). The value of fuzzy membership is exhibited by the

yellow part under the Gaussian curve. The blue lines in the third column show the proximity of predicted values to experimental values.

R^2 values of both components were determined to investigate the goodness of fit of this model (Fig. 7). R squared was found to be 0.9988 and 0.9978 for TAM and DTS, respectively. These

Fig. 7 Predicted values versus actual values of TAM and DTS in FIS model



results indicate a relatively good closeness of the predicted values to the actual values. As shown in Table 4, the acceptable range of recovery percentage

Table 4 Recovery, mean recovery, and RMSE of mixture analysis by FIS for both components

| Actual (µg/L) | | Predicted (µg/L) | | Recovery (%) | |
|-------------------|-----|------------------|------|--------------|--------|
| TAM | DTS | TAM | DTS | TAM | DTS |
| 50 | 50 | 50 | 50 | 100.00 | 100.00 |
| 200 | 50 | 195 | 52.8 | 97.50 | 105.60 |
| 150 | 80 | 150 | 80 | 100.00 | 100.00 |
| 80 | 100 | 81 | 106 | 101.25 | 106.00 |
| 200 | 100 | 193 | 105 | 96.50 | 105.00 |
| 100 | 150 | 98 | 147 | 98.00 | 98.00 |
| 50 | 200 | 50 | 200 | 100.00 | 100.00 |
| 200 | 200 | 200 | 199 | 100.00 | 99.50 |
| Mean recovery (%) | | | | 99.15 | 101.76 |
| RMSE | | | | 3.1425 | 3.1393 |

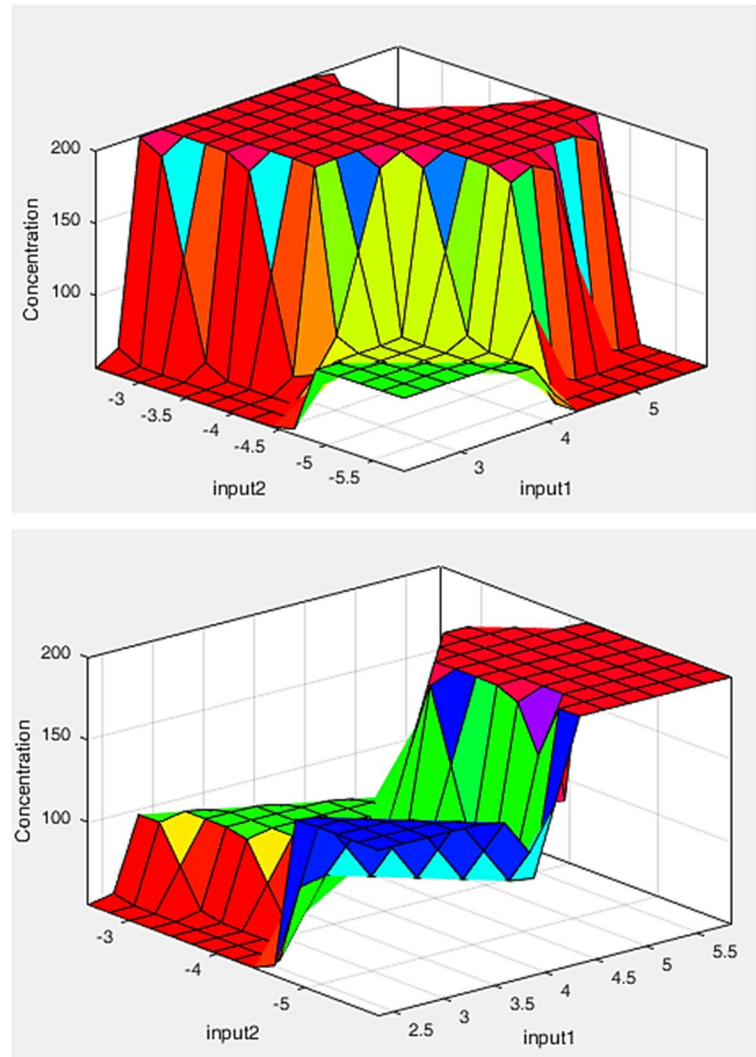
(TAM=96.5–101.25% and DTS=98.00–106.00%) and mean recovery percentage (TAM=99.15% and DTS=101.76%) indicated appropriate accuracy of FIS model. Relatively low RMSE (TAM=3.1425 and DTS=3.1393) expresses the good performance of the proposed method.

The correlation between input 1, input 2, and output (concentration) is illustrated with a three-dimensional (3D) surface view (Fig. 8). These inputs possess an important role in the prediction of concentrations.

Linear range of calibration curves

The change of color from red to blue related to the AuNPs-TAM and AuNPs-DTS solutions can be easily observed by the bare eyes (Fig. 9a). The calibration curves were obtained in a linear range of 50–200 µg/L for both components. The calibration equations of TAM and DTS

Fig. 8 Surface view of correlation between input 1, input 2, and output in the FIS model for TAM and DTS



were $y=0.0001x+0.1591$ with $R^2=0.9958$ and $y=0.0008x+0.1676$ with $R^2=0.9912$, respectively (Fig. 9b and c). The limit of detection (LOD) and limit of quantification (LOQ) were calculated using Eqs. (2) and (3), respectively.

$$\text{LOD} = 3.3\sigma/S \quad (2)$$

$$\text{LOQ} = 10\sigma/S \quad (3)$$

where, σ and S are the standard deviation of the response and the slope of the calibration curve, respectively [32]. LOD was obtained at 21.08 and

21.82 $\mu\text{g/L}$ for TAM and DTS, respectively. Also, LOQ was found to be 66.12 and 63.90 $\mu\text{g/L}$ for TAM and DTS, respectively.

HPLC results

Analysis of the Avolosin capsule containing 0.4 mg TAM and 0.5 mg DTS was accomplished using the HPLC technique. Its chromatogram revealed that the retention time of DTS and TAM was 10.546 min and 19.128 min, respectively (Fig. 10).

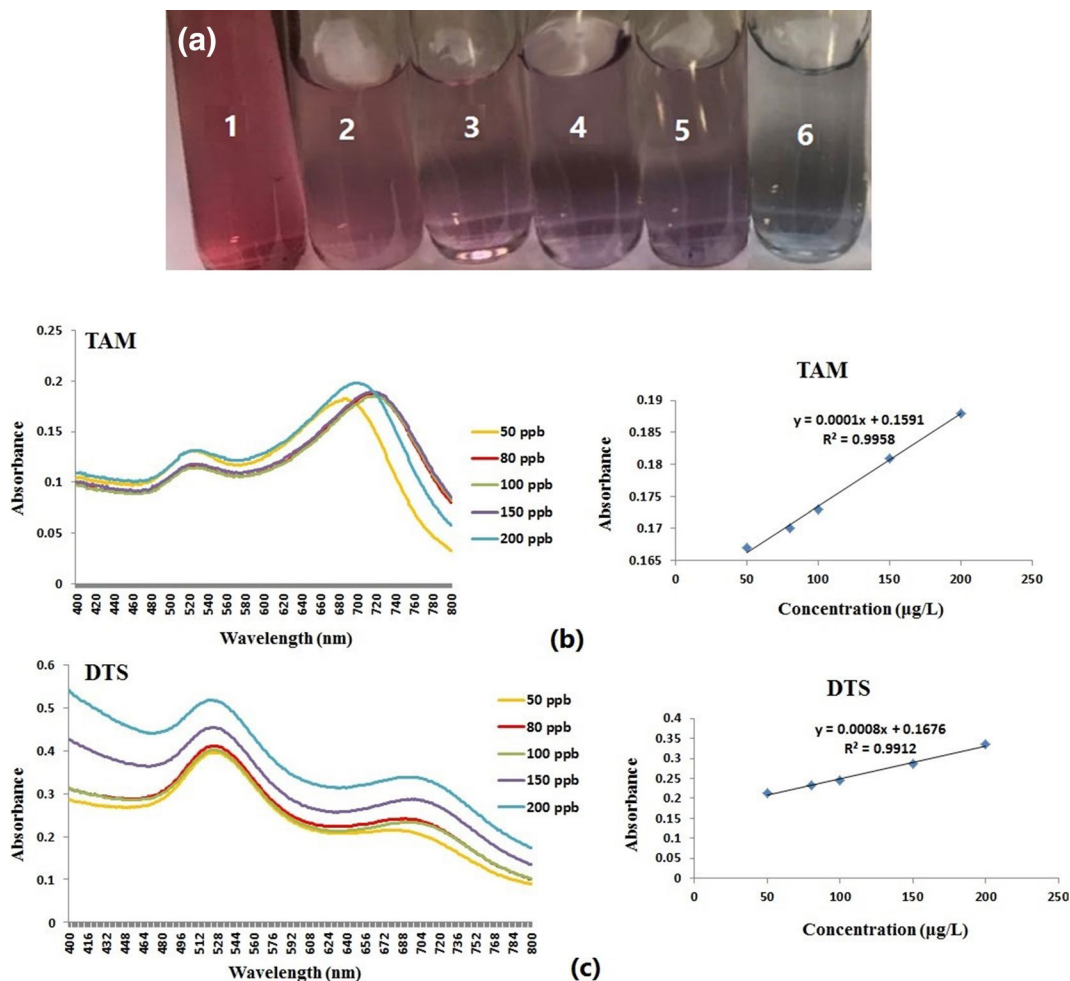


Fig. 9 a Photographs showing colorimetric images of AuNPs-drug with different concentrations of TAM and DTS 1: 0, 2: 50, 3: 80, 4: 100, 5: 150, 6: 200. b, c UV-Vis spectra and calibration curves of the AuNPs-TAM and AuNPs-DTS

Real sample analysis

The applicability of the suggested methods and HPLC was assessed by analyzing the pharmaceutical sample for the simultaneous determination of TAM and DTS (Table 5). The closeness of the values obtained by the proposed methods and the values on the label claim of the commercial capsule is clearly evident in the results. The mean recovery percentage of TAM for RBF and FIS was 96.91% and 94.08%, respectively, whereas the relative standard deviation (RSD) was lower than 1.5%. On the other hand, the

mean recovery percentage of DTS was achieved at 96.33% and 95.06% for RBF and FIS, respectively, while RSD was < 1%. The precision of these methods was proved by the low RSD values. The obtained results demonstrated the potential applicability of these models for the concurrent estimation of TAM and DTS in real samples.

The results obtained from the RBF and FIS were compared with HPLC using the ANOVA test (Table 6). The smaller calculated *F* values (TAM: 0.489108 and DTS: 0.105180) proved the absence of significant differences between the methods.

Fig. 10 Obtained chromatogram from the commercial formulation of Avolosin containing TAM and DTS

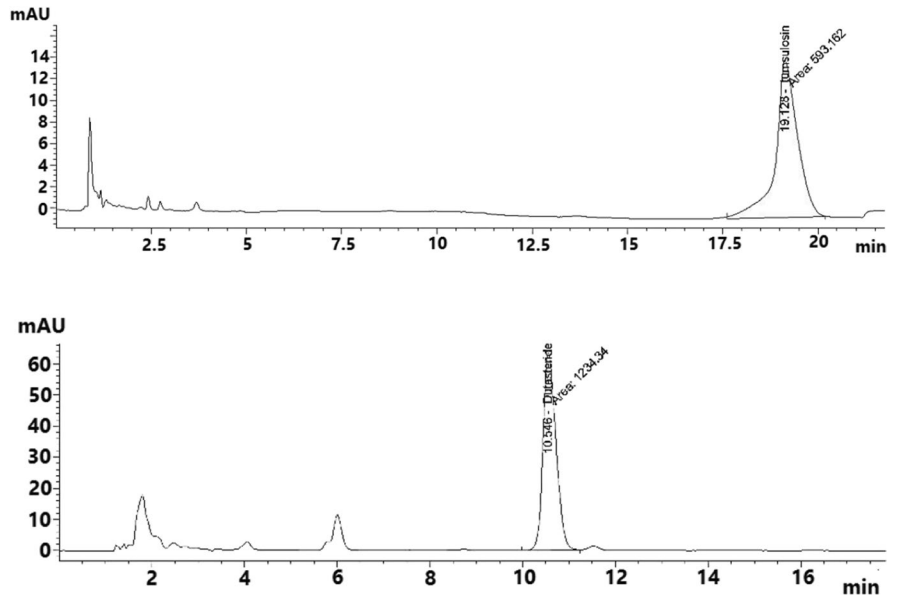


Table 5 Results of analyzing Avolosin by the proposed and reference methods (0.4 mg TAM and 0.5 mg DTS in pharmaceutical formulation)

| TAM | DTS | | | | | |
|-------------------------|--------|--------|--------|--------|--------|--------|
| | RBF | FIS | HPLC | RBF | FIS | HPLC |
| Found ^a (mg) | 0.3876 | 0.3763 | 0.3766 | 0.4816 | 0.4753 | 0.4733 |
| Mean recovery (%) | 96.91 | 94.08 | 94.16 | 96.33 | 95.06 | 94.66 |
| SD | 0.0035 | 0.005 | 0.005 | 0.0030 | 0.0045 | 0.0115 |
| RSD (%) | 0.9043 | 1.329 | 1.515 | 0.6237 | 0.9473 | 2.325 |

^aMean value of the three measurements

Table 6 Statistical analysis using ANOVA test

| Source of variation critical | SS ^a | df ^b | MS ^c | F calculated | F |
|------------------------------|-----------------|-----------------|-----------------|--------------|----------|
| Between groups | | | | | |
| TAM | 5.4888E-05 | 2 | 2.7444E-05 | 0.489108 | 5.143252 |
| DTS | 1.4888E-05 | 2 | 7.4444E-06 | 0.105180 | 5.143252 |
| Within groups | | | | | |
| TAM | 0.0003366 | 6 | 5.6111E-05 | | |
| DTS | 0.0004246 | 6 | 7.0777E-05 | | |
| Total | | | | | |
| TAM | 0.0003915 | 8 | | | |
| DTS | 0.0004395 | 8 | | | |

^aSum of squares

^bDegree of freedom

^cMean squares

Table 7 Comparison of the proposed method with some of the previously reported methods for the simultaneous determination of TAM and DTS

| Method | Real sample | Linear range ($\mu\text{g/L}$) | LOD ($\mu\text{g/L}$) | LOQ ($\mu\text{g/L}$) | Ref. |
|-------------------|-----------------------|--|------------------------------------|------------------------------------|------------|
| RP-HPLC | Pharmaceutical dosage | 5×10^4 – 1.5×10^5 | TAM:170 DTS:210 | TAM:520 DTS:650 | [10] |
| RP-HPLC | Pharmaceutical dosage | TAM: 1.92×10^4 – 4.48×10^4 DTS: 2.4×10^4 – 5.6×10^4 | TAM:740 DTS:1290 | TAM:2240 DTS:3910 | [11] |
| RP-HPLC | Pharmaceutical dosage | 2.5×10^4 – 1.25×10^5 | --- | --- | [33] |
| RP-HPLC | Pharmaceutical dosage | 6×10^4 – 1×10^5 | --- | --- | [34] |
| Spectrophotometry | Pharmaceutical dosage | 1000– 30×10^4 | TAM: 2.6×10^4 DTS:2600 | TAM: 7.9×10^4 DTS:7900 | [35] |
| Colorimetry | Pharmaceutical dosage | 50–200 | TAM:21.08 DTS:21.82 | TAM:63.90 DTS:66.12 | This study |

Comparison with other methods

A comparison between the results obtained by the present method and those achieved by other techniques for the simultaneous determination of TAM and DTS was given in Table 7. It can be stated that the colorimetric method has a good linear range, LOD, and LOQ compared to the obtained from the other approaches.

Conclusion

In this study, a novel and simple colorimetric method based on surface plasmon resonance along with chemometric methods (RBF and FIS) were developed for the simultaneous determination of two drugs (tamsulosin and dutasteride) in their pharmaceutical formulations using AuNPs. The synthesized AuNPs represented a colorimetric response upon exposure to the pharmaceutical formulation containing TAM and DTS, which was related to the SPR feature and aggregation of AuNPs. The aggregation of AuNPs induced by the drug was confirmed by TEM and DLS, which results in a change in absorption spectra (524 to 674 nm) and in color (red to gray). RBF-NN and FIS models produced accurate results, and the RSD was almost lower than 1% and 1.5% for RBF and FIS, respectively. This colorimetric approach revealed low LOD and LOQ for the TAM and DTS. It was successfully used to determine two drugs in the Avolosin capsule, which

indicates that this proposed method possesses a high potential for the simultaneous detection of TAM and DTS in the pharmaceutical sample. In comparison with available analytical techniques for simultaneous estimation of TAM and DTS, the suggested method had some advantages, including needing smaller amounts of reagents, being easy, rapid, and inexpensive, and it does not require any costly apparatus.

Author contribution The first draft of the manuscript was written by Ghasem Mahmoudi. Experimental and software sections were performed by Ghasem Mahmoudi. The manuscript was edited by Mahmoud Reza Sohrabi. Data review was done by Fereshteh Motiee.

Data availability The datasets generated are available from the corresponding author on reasonable request.

Declarations

Ethics approval In this study, no ethical approval is required.

Consent for publication There is no human research in this study.

Conflict of interest The authors declare no competing interests.

References

- Lulic Z, Son H, Yoo SB, Cunningham M, Kapse P, Miller D, Cortes V, Park S, Bhak RH, Sheng Duh M (2021) Free combination of dutasteride plus tamsulosin for the treatment of benign prostatic hyperplasia in South Korea: analysis of drug utilization and adverse events using the

- National Health Insurance Review and Assessment Service database. *BMC Urol* 21:178
2. Hakak Zade E, Mollahosseini A (2021) Application of reusable flat-membrane in electro-membrane extraction for tamsulosin hydrochloride determination in cleaning validation samples of sterile production line equipment by RP-HPLC. *Eur J Pharm Sci* 161:105793
 3. Tavooasian A, Oliveira Reis L, Aluru P, Khajavi A, Kazem Aghamir SM (2022) Comparison of tamsulosin and tadalafil effects in LUTS treatment considering patients' atherosclerosis risk level. *Ann Med Surg* 80:104137
 4. Nandana PI, Adipura LR, Rasyid H (2021) The effect of tamsulosin and dutasteride combination drug therapy on prostate volume in patients with benign prostatic hyperplasia. *IOP Conf. Series: Earth Environ Sci* 712: 012024
 5. Giriraj P, Sivakkumar T (2017) Simultaneous estimation of dutasteride and tamsulosin hydrochloride in tablet dosage form by Vierordt's method. *Arab J Chem* 10:S1862–S1867
 6. Wu C, Kapoor A (2013) Dutasteride for the treatment of benign prostatic hyperplasia. *Expert Opin Pharmacother* 14:1399–1408
 7. Patel DB, Patel NJ, Patel SK, Prajapati AM, Patel SA (2010) RP-HPLC Method for the estimation of dutasteride in tablet dosage form. *Indian J Pharm Sci* 72:113–116
 8. Higazy A, Shorbagy AA, Shabayek M, Radwan A, Halim GN, Osman D, Osman T (2022) Short course of dutasteride in treatment of a refractory category IIB chronic prostatitis (a placebo-controlled study). *Prostate International* 10:213–217
 9. Lopes Ciríaco S, Pereira Santos Carvalho I, Alves Terceiro Neto J, Sousa Lima Neto J et al (2020) Development of microemulsion of tamsulosin and dutasteride for benign prostatic hyperplasia therapy. *Colloids Surfaces B: Biointerfaces*. 185:11057
 10. Mohammed Ishaq B, Vanitha Prakash K, Krishna Mohan G (2014) Simultaneous determination of dutasteride and tamsulosin in pharmaceutical dosage forms by RP-HPLC. *Der Pharma Chemica* 6:103–109
 11. Ahmed SH, Karunakranth D, Sridhar Babu R, Khasim SM, Arbaaz Khan M, Ghouse S, Aizaz Ehsan S, Fatima N, Pasha S (2019) To develop new RP HPLC method for the simultaneous estimation of tamsulosin hydrochloride and dutasteride in pharmaceutical dosage form. *J Drug Dev Delivery* 2:7–12
 12. Abbas AE, Eid SM, Serag A, Attia KAM (2021) A validated TLC-densitometry for the simultaneous determination of tamsulosin and dutasteride in their combined pharmaceutical formulation. *Al-Azhar J Pharmaceut Sci* 64:93–107
 13. Monir HH, Ali AM, Refat RE, Abbas SS (2020) Chromatographic methods for determination of finasteride and tamsulosin hydrochloride and in presence of finasteride degradation product. *Acta Chromatogr* 32:95–101
 14. Agarwal S, Veeran Gowda K, Kanti Sarkar A, Ghosh D, Bhaumik U, Kumar Chattaraj T, Kumar Pal T (2008) Simultaneous determination of tamsulosin and dutasteride in human plasma by LC–MS–MS. *Chromatographia* 67:893–903
 15. Becze A, Alexandra Resz M, Ilea A, Cadar O (2022) A validated HPLC multichannel DAD method for the simultaneous determination of amoxicillin and doxycycline in pharmaceutical formulations and wastewater samples. *Appl Sci* 12:9789
 16. Rodrigues M, Alves G, Ferreira A, Queiroz J, Falcaõ, A. (2013) A rapid HPLC method for the simultaneous determination of amiodarone and its major metabolite in rat plasma and tissues: a useful tool for pharmacokinetic studies. *J Chromatogr Sci* 51:361–370
 17. Chen Chang C, Pein Chen C, HengWu T, Hsu Yang C, Wann Lin C, Chen CY (2019) Gold nanoparticle-based colorimetric strategies for chemical and biological sensing applications. *Nanomaterials* 9:861
 18. Kim K, Nam YS, Lee Y, Lee KB (2017) Highly sensitive colorimetric assay for determining Fe³⁺ based on gold nanoparticles conjugated with glycol chitosan. *J Anal Methods Chem* 2017:3648564
 19. Wu S, Li D, Wang J, Zhao Y, Dong S, Wang X (2017) Gold nanoparticles dissolution based colorimetric method for highly sensitive detection of organophosphate pesticides. *Sens Actuators B* 238:427–433
 20. Liu G, Lu M, Huang X, Li T, Xu D (2018) Application of gold-nanoparticle colorimetric sensing to rapid food safety screening. *Sensors* 18:4166
 21. Shahbazi N, Zare-Dorabei R (2019) A facile colorimetric and spectrophotometric method for sensitive determination of metformin in human serum based on citrate-capped gold nanoparticles: central composite design optimization. *ACS Omega* 4:17519–17526
 22. Jazayeria MH, Aghaie T, Avan A, Vatankhah A, Ghaffari MRS (2018) Colorimetric detection based on gold nanoparticles (GNPs): an easy, fast, inexpensive, low-cost and short time method in detection of analytes (protein, DNA, and ion). *Sens Bio-Sens Res* 20:1–8
 23. Alhaj Sakur A, Zakri AL, D. (2022) A new selective colorimetric method coupled with a high-resolution UV method for the consecutive quantification of three drugs in semi-solid preparations. *Heliyon* 8:e11003
 24. Määttä J, Bazaliy V, Kimari J, Djurabekova F, Nordlund K, Roos T (2021) Gradient-based training and pruning of radial basis function networks with an application in materials physics. *Neural Netw* 133:123–131
 25. Vema V, Sudheer KP, Chaubey I (2019) Fuzzy inference system for site suitability evaluation of water harvesting structures in rainfed regions. *Agric Water Manag* 218:82–93
 26. Liu Y, Zhao M (2022) An obsolescence forecasting method based on improved radial basis function neural network. *Ain Shams Eng J* 13:101775
 27. Famelis I, Donas A, Galanis G (2022) Comparative study of FeedForward and radial basis function neural networks for solving an environmental boundary value problem. *Results Appl Math* 16:100344
 28. Nayak PC, Sudheer KP, Ramasastri KS (2005) Fuzzy computing based rainfall–runoff model for real time flood forecasting. *Hydrol Process* 19:955–968
 29. Mamdani EH, Assilian S (1975) An experiment in linguistic synthesis with a fuzzy logic controller. *Int J Man Mach Stud* 7:1–13
 30. Takagi T, Sugeno M (1985) Fuzzy identification of systems and its applications to modeling and control. *IEEE Transactions on Systems, Man, and Cybernetics*. SMC-15: 116–132

31. Elmi Z, Faez K, Goodarzi M, Goudarzi N (2009) Feature selection method based on fuzzy entropy for regression in QSAR studies. *Mol Phys* 107:1787–1798
32. Sohrabi MR, Darabi G (2016) The application of continuous wavelet transform and least squares support vector machine for the simultaneous quantitative spectrophotometric determination of myricetin, kaempferol and quercetin as flavonoids in pharmaceutical plants. *Spectrochim Acta Part A Mol Biomol Spectrosc* 152:443–452
33. Sravan Kumar Reddy G, Ashutosh Kumar S, Debnath M, Raj Kumar V (2014) Analytical method development & validation for simultaneous determination of dutasteride and tamsulosin in bulk as well as in pharmaceutical dosage form by using RP-HPLC. *Int J Pharm Pharmaceut Sci* 6:77–84
34. Srilatha U, Kumar A (2020) Method development and validation of dutasteride and tamsulosin by RP-HPLC. *Int J Sci Res Method* 14:93–103
35. Bin Sayeed K, Rizwan Sh, Begum H (2015) Development and validation of stability indicating method for the simultaneous determination of tamsulosin and dutasteride in bulk drugs and pharmaceutical dosage forms using UV spectrophotometric method. *Int J Res Dev Pharm Life Sci* 4:1434–1446

Publisher's Note Springer Nature remains neutral with regard to jurisdictional claims in published maps and institutional affiliations.

Springer Nature or its licensor (e.g. a society or other partner) holds exclusive rights to this article under a publishing agreement with the author(s) or other rightsholder(s); author self-archiving of the accepted manuscript version of this article is solely governed by the terms of such publishing agreement and applicable law.